

# A slow and dark atomic beam

B. K. Teo, T. Cubel, G. Raithel

*FOCUS Center and Physics Department, University of Michigan, 500 East  
University, Ann Arbor MI 48109, USA.*

---

## Abstract

We demonstrate a method to produce a very slow atomic beam from a vapour cell magneto-optical trap. Atoms are extracted from the trap using the radiation pressure imbalance caused by a push beam. An additional transfer beam placed near the center of the trap transfers the atomic beam into an off-resonant state. The velocity of the atomic beam has been varied by changing the intensity of the push beam or the position of the transfer beam. The method can be used to generate a continuous, magnetically guided atomic beam in a dark state.

*Key words:* MOT, atom guides, atomic beams, laser cooling

*PACS:* 32.80.Pj, 42.50.Vk, 03.75.-b

---

## 1 Introduction

Cold atomic beams are useful for atom interferometry and precision atomic spectroscopy experiments. Cold beams were first derived from oven sources and slowed by the radiation pressure from a resonant laser beam which can be temporally chirped [1] or operated at fixed frequency in conjunction with Zeeman coils [2]. These atomic beams have a large transverse velocity spread because the atoms are cooled in only one dimension. Colder atomic beams that are both transversely and longitudinally cooled can be derived from 2D magneto-optical traps (MOTs) and moving optical molasses [3–6]. The mean beam velocity produced by these 2D MOTs is tunable between 0.5–3 m/s. Atoms can also be extracted from 3D MOTs using the Low Velocity Intense Source (LVIS) geometry, in which a radiation pressure imbalance is created by a small hole at the center of one of the retro-reflecting mirror-waveplate assemblies [7], or by an additional laser beam [8,9]. These sources produce atomic beams with a mean velocity of about 15 m/s. Recently, the propagation of cold atomic beams in magnetic guides has been studied [10–13].

Evaporative cooling of transversely confined atomic beams is a promising route towards the generation of a continuous source of Bose Einstein Condensates (BEC) [14]. This approach to a continuous coherent atom source differs from the method of periodic replenishment of a static BEC reservoir [15], where suitably interlaced moving optical dipole traps are used. In the latter method, large number and phase fluctuation of the condensate can be expected. The phase and atom number will be more stable if the whole system runs continuously, without moving potentials and/or pulsed atomic beams. A BEC continuously replenished by an evaporatively cooled, guided atomic beam should therefore have much lower phase and atom number variations.

Evaporative cooling of a magnetically guided atomic beam presents technical challenges. To achieve high enough densities and collision rates, a very large flux of cold atoms (better than  $10^9 \text{ s}^{-1}$ ) moving at very low velocities (less than 1 m/s) is required. The atomic flux must be in a low-field-seeking state and must be efficiently coupled into the guide. These challenges can only be partially met when using the beam sources described in [7–9], which produce atomic beams with longitudinal velocities of order 15 m/s. Moving optical molasses combined with magneto-optic trapping can produce dense, guided atomic beams with velocities in the 1 m/s range [16]. Other schemes to couple cold atoms into magnetic guides have been studied in [12,13].

The simultaneous operation of a MOT producing an atomic beam and a nearby magnetic atomic-beam guide is a further challenge. In such a system, the MOT will produce some stray light in its vicinity. The MOT stray light will be scattered by the atoms propagating in the atom guide, resulting in optical pumping of the atoms out of the desired low-field-seeking magnetic sublevel. Stray light intensities  $< 1 \text{ nW/cm}^2$  of near-resonant light (for Rb atoms) will seriously attenuate the magnetically guided atomic beam. It appears very hard to suppress the MOT stray light below that intensity level. A promising way out of this dilemma is to optically pump the atomic beam emitted from the MOT into a dark, low-field-seeking state before the near-resonant stray light from the MOT depletes it. In alkali atoms, a magnetic sublevel of the lower of the two ground-state hyperfine levels can be used as such a dark state. To ensure a rapid enough transfer into that state, a separate optical-pumping laser can be used. In this paper, we use this idea to produce a slow beam of  $^{87}\text{Rb}$  atoms in the  $|F = 1, m_F = -1\rangle$  ground-state sublevel, which is dark with respect to the stray light of a nearby MOT (which is the atomic-beam source). In addition to being in a dark state, the atomic beam is also considerably slower than the bright atomic beams in [7–9]. Experimental data from pulsed measurements are shown, but the method can also generate continuous, dark atomic beams. The beam may be magnetically guided and, in future efforts, evaporatively cooled while the MOT is operating.

## 2 Extraction of Atoms from a Vapour Cell MOT

We use a six-beam vapour-cell MOT and a push laser to produce a  $^{87}\text{Rb}$  atomic beam. The radiation pressure imbalance due to the push beam [8,9] accelerates cold atoms out of the center of the MOT. The MOT and pusher beams act on the upper hyperfine level  $F = 2$  of  $^{87}\text{Rb}$ . The velocity of the resultant atomic beam is determined by the intensity, detuning, and polarization of the push laser. Since the Zeeman and the Doppler shifts of the atoms are position- and/or velocity-dependent, the acceleration also depends on position and velocity. On average, a  $^{87}\text{Rb}$  atom extracted from the MOT scatters about 10,000 photons from the push beam before it is pumped into the lower hyperfine state  $F = 1$  via an accidental off-resonant  $F = 2 \rightarrow F' = 2$  transition. The acceleration phase of the atom can, however, be terminated early using an additional laser beam, referred to as transfer beam, that optically pumps the atom into the  $F = 1$  ground state. Because of the large energy spacing between the  $F = 1$  and  $F = 2$  ground states, the push and the MOT light is not resonant with the  $F = 1$  atoms. The dark atomic beam is slower than that produced by a conventional LVIS. Also, *all* atoms in the beam cease accelerating at the same location, namely when they enter the transfer beam. This fact leads to a velocity spread of the dark atomic beam that is less than the velocity spread of a conventional LVIS atomic beam.

The repumper light required to operate the MOT is resonant with the  $F = 1 \rightarrow F' = 2$  transition and must therefore be sufficiently shielded from the  $F = 1$  dark atomic beam. There is only a single MOT repumper beam, and that beam has a low intensity and is quite small. Therefore, it is technically *much* easier to shield the repumper stray light from the dark atomic beam than preventing the MOT stray light, which is near-resonant with the  $F = 2 \rightarrow F' = 3$  transition, from reaching the atomic beam. This (practical) difference in the ability to shield MOT stray light from the atomic beam vs. the ability to shield repumper stray light has been a major motivation for the development of the method presented in this paper.

## 3 Experimental Setup

Our experimental setup has been described previously in [17] and is shown schematically in Fig. 1. We use a two-wire magnetic atom guide. The guide wires are separated by 2.8 cm and are placed outside a quartz vacuum tube. The transverse magnetic field of the atom guide varies along the guide axis ( $z$  direction) due to the presence of two tapered pieces of magnetic iron. At a current of 400 A, the transverse magnetic field gradient increases from 70 G/cm to 320 G/cm along the guide.  $^{87}\text{Rb}$  atoms are captured from the background

gas in a MOT, which is formed on the axis of the guide. The MOT laser beams are detuned by a frequency of  $2\Gamma/2\pi = 12$  MHz to the red of the  $5S_{1/2}F = 2 \rightarrow 5P_{3/2}F' = 3$  transition and have an intensity of  $5 \text{ mW/cm}^2$ . An additional beam resonant with the  $5S_{1/2}F = 1 \rightarrow 5P_{3/2}F' = 2$  repumps atoms that fall into the  $F = 1$  state back into  $F = 2$ . In our pulsed experiments, during the MOT loading phase the guide current is reduced to 200 A, and a pair of external magnetic coils is energized, resulting in a MOT magnetic field with gradients -15, 26 and -11 G/cm in the  $x, y$  and  $z$  directions. In each loading cycle,  $2 \times 10^7$  atoms are collected by the MOT.

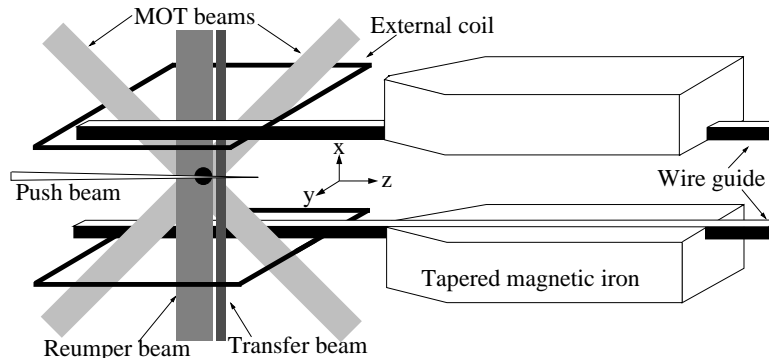


Fig. 1. Schematic of our magnetic guide setup. The vacuum chamber (not shown) rests in between and parallel to the wire guide. The magnetic iron is tapered to give a smooth change in transverse field gradient along the guide axis.

Cold atoms are extracted from the MOT using a push laser beam propagating along the guide axis [8,9]. In the presented experiments, the guide current (see Fig. 1) is increased from 200 A to 400 A at the time when the push laser beam turns on, while the current in the external coils is kept constant. The push beam has the same detuning as the six MOT beams and produces a radiation pressure imbalance at the MOT center that forces the atoms out. The MOT repumper beam intersects the  $z$ -axis at a right angle and is masked by a sharp edge such that the repumper intensity abruptly drops to zero a few mm downstream from the MOT (see Fig. 1). The transfer beam, located close to the MOT, optically pumps the extracted atoms into the  $F = 1$  dark state. The transfer beam is locked to the  $5S_{1/2}F = 2 \rightarrow 5P_{3/2}F' = 2$  transition. The transfer beam has a circular cross section (diameter of  $\approx 2$  mm) with an approximately constant intensity equal to the saturation intensity ( $I_{\text{sat}} = 1.6 \text{ mW/cm}^2$ ). The transfer beam interrupts the acceleration of the atoms. While providing a well defined location of transfer from  $F = 2$  to  $F = 1$ , repeated transitions of the atoms back and forth between these states must be avoided. Therefore, any spatial overlap between the repumper and the transfer beam needs to be avoided.

In our experiments we have, for convenience, used an existing small uncoated quartz cell as our vacuum chamber. Therefore, the amount of stray light present in the vacuum system has been unusually high. In order to reduce

the amount of repumper stray light in the atom guiding region to an acceptable level, the MOT repumper intensity had to be reduced to levels so low that the number of atoms in the MOT has been significantly reduced. Obviously, a larger vacuum chamber with dark surfaces and vacuum windows placed outside direct line-of-sight from the guided atoms will allow us to use a higher MOT repumper intensity.

## 4 Experimental Data

To detect the fluorescence of the atomic beam, the beam is imaged onto a 3 mm by 3 mm photodiode (magnification approximately one). The center of the photodiode corresponds to an object location that has a distance of 1 cm from the MOT center. To measure the time-of-flight distribution of the atomic beam, a mechanical shutter is used to pulse the push beam. The onset of the push beam extracts a pulse of atoms from the MOT. The MOT beams can be turned off or left on continuously during the extraction. The extracted atoms stream through the region that is imaged onto the photodiode. Atoms that enter the detection region in the state  $F = 2$  are still being accelerated by the push beam. The resultant fluorescence is detected, and its time-dependence can be used as a measure for the average velocity and velocity spread of the atoms. To be able to also detect atoms propagating in the dark state ( $F = 1$ ), an additional repumping beam can be introduced into the detection region. This repumper returns atoms propagating in the dark state  $F = 1$  into the bright state  $F = 2$ , thereby making them detectable.

### 4.1 Pulsed Measurements of Velocity

The following data shows the time dependence of the fluorescence signal for the case that the leading edge of the transfer beam is located 3 mm from the MOT. The MOT beams are shut off before the push beam is turned on. Without the transfer beam, most of the atoms remain in the  $F = 2$  bright state and scatter light from the push beam (solid curve in Fig. 2) while accelerating. Assuming constant acceleration we find, based on the average arrival time of the atoms, an average velocity of the atoms of about 10 m/s. When the transfer beam is turned on and the additional repumper in the detection region is left off, most of the atoms are pumped into the  $F = 1$  dark state and traverse the detection region undetected. The weak remnant signal in Fig. 2 corresponds to a small fraction of atoms that are still in the bright state  $F = 2$ . The presence of those atoms is due to stray repumper light throughout the chamber that accidentally returns some atoms from the dark into the bright state before they leave the detection region.

The dashed curve in Fig. 2 shows the signal observed when both the transfer beam and the additional repumper beam in the detection region are used. In that case, the acceleration of the atoms is suspended at the leading edge of the transfer beam, and resumes at the leading edge of the repumper beam in the detection region. The fluorescence associated with the renewed acceleration is measured. The peak of this signal is delayed by 0.4 ms with respect to the signal measured without transfer beam. Assuming that the transfer beam is located approximately 3 mm from the MOT, from the observed delay of 0.4 ms we deduce an average velocity of the dark beam of about 5 m/s. This is more than a factor of two slower than any atomic beam based on the LVIS design. The velocity of the dark atomic beam can be controlled by the intensity of the push beam as well as the distance of the transfer beam from the MOT center. We demonstrate this in the next two sections.

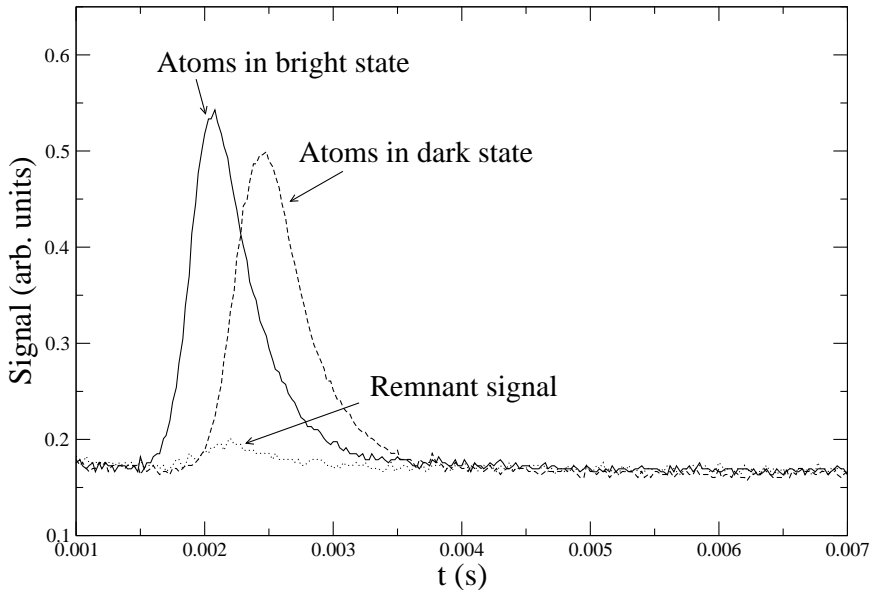


Fig. 2. Time-resolved measurements of the fluorescence of a pulsed atomic beam at a distance of 1 cm from the MOT. The push beam is turned on at  $t = 0$ . The solid curve is the signal without the transfer beam. When the transfer beam is turned on, most atoms are pumped into the dark state and do not fluoresce; the small fraction of atoms left in the bright state produce a weak remnant signal (dotted curve). In the dashed curve, an additional repumper beam in the detection region is used to pump the atoms in the dark state back into the bright state. The delay between the solid and dashed curves reflects the velocity difference between the bright and dark atomic beams.

## 4.2 *Effect of the Push Beam Intensity*

In the following, we discuss a series of fluorescence measurements obtained for various push beam intensities. The rising edge of the transfer beam is located 3 mm from the MOT center. The MOT beams are always on, and the radiative force of the pulsed push beam must overcome the damping force of the MOT to extract the atoms. We find that for a given push beam intensity the push beam is most effective if it is  $\sigma$ -polarized, with a helicity that is opposite to that one would use if the pusher beam was a MOT trap beam. Under this condition, the magnetic field of the MOT tunes the atoms closer to resonance with the push beam as they are pushed out from the MOT, resulting in a larger acceleration. We have also found that for the push beam to overcome the damping force of the MOT, the push beam power must exceed a threshold power of about 0.1 mW. Below this power, the push beam merely displaces the MOT, and there is no atomic beam.

Fig. 3(a) shows the fluorescence signal for different values of the push beam power when both the transfer beam and the additional repumper laser in the detection region are turned on. As the push beam power decreases, the fluorescence signal peaks at later times, corresponding to a lower average beam velocity. For each push beam power, we have, for comparison, also measured the fluorescence signals without transfer laser (data not shown). For the resultant pairs of curves, one pair being analogous to the solid and the dashed curve of Fig. 1, we have then determined the difference in the most probable arrival time of the atoms. In Fig. 3(b), the time differences are plotted vs. push beam power. With decreasing power, the delay time between the transfer-on and transfer-off signals increases from 0.02 ms to 1.00 ms. This behavior reflects the fact that the time of travel of the dark atomic beam from the transfer beam to the detection region increases with decreasing velocity.

## 4.3 *Effect of the Transfer Beam Position*

The velocity of the dark atomic beam can also be controlled by varying the position of the transfer beam relative to the MOT center. Moving the transfer laser closer to the MOT leaves the atoms less time to interact with the push beam before they are pumped into the dark state. This results in a slower dark atomic beam. Fig. 4 shows the fluorescence signal, with both the transfer beam and the additional repumper beam on, for three distances of the transfer beam from the MOT. As explained in Sec. 3 and in Fig. 1, the cutoff of the MOT repumper beam and the transfer beam need to be varied such that there always remains a small gap between both beams. As expected, the delay time caused by the transfer beam increases when the transfer beam is moved

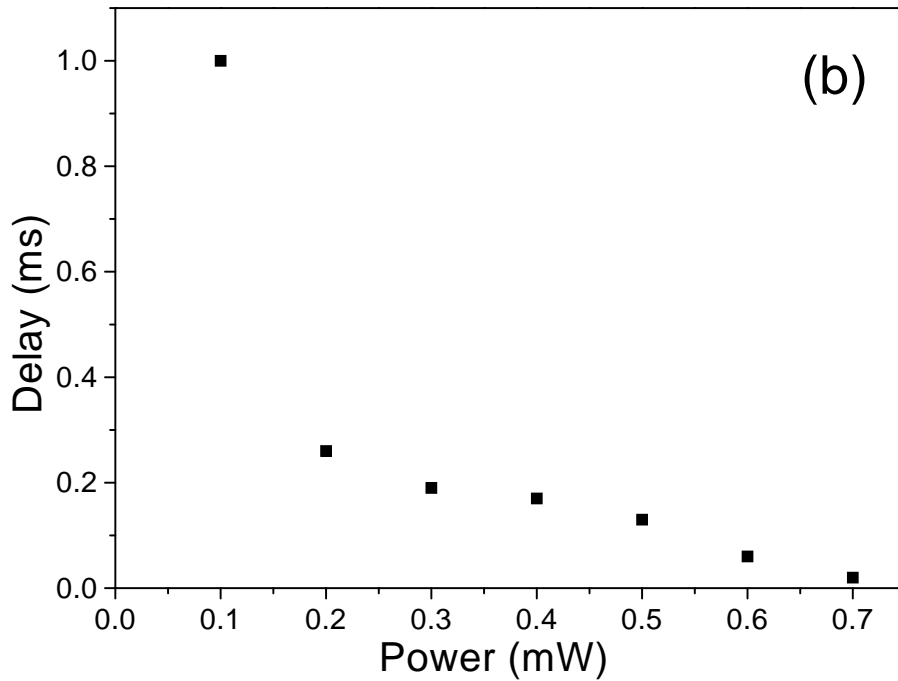
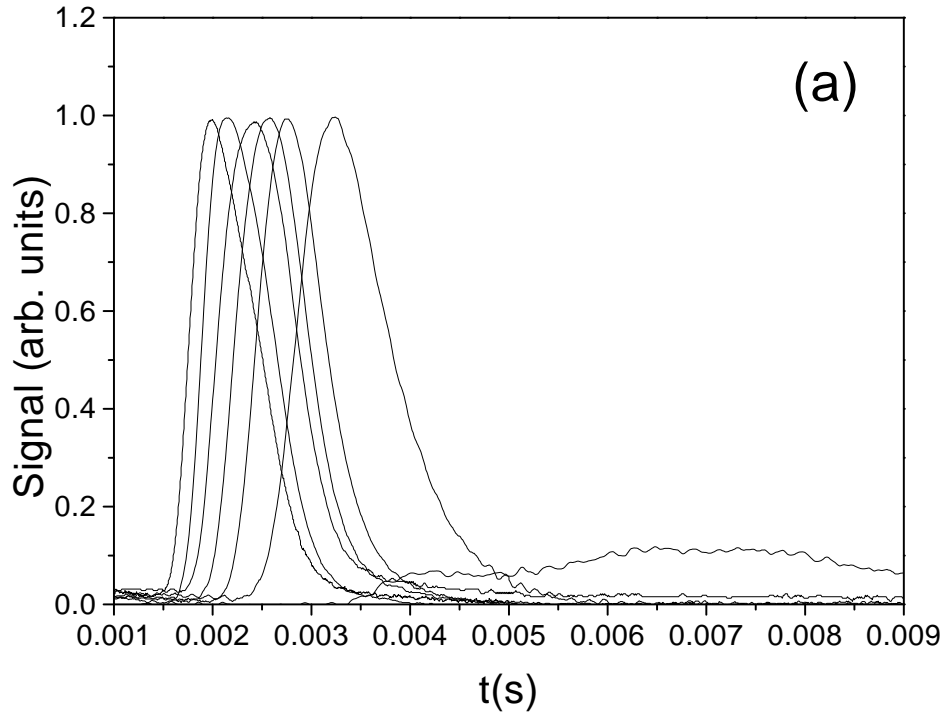


Fig. 3. (a) Fluorescence signals of pulsed atomic beams for push beam powers ranging from 0.1 mW to 0.7 mW (right to left in steps of 0.1 mW). The push beam diameter is 2 mm. Both the transfer laser and the additional repumper laser in the detection region are turned on. A minimum power of 0.1 mW is needed to extract atoms. (b) Delay of most probable arrival time of atoms due to effect of the transfer beam versus the power of the push beam.



towards the MOT. There is a tradeoff between attaining a large atom flux and a low atomic-beam velocity. While moving the transfer laser beam closer to the MOT results in a slower atomic beam (which may be desired), it also entails the necessity to move the MOT repumper cutoff closer to the MOT center, thereby decreasing the MOT loading efficiency and the atomic-beam flux.

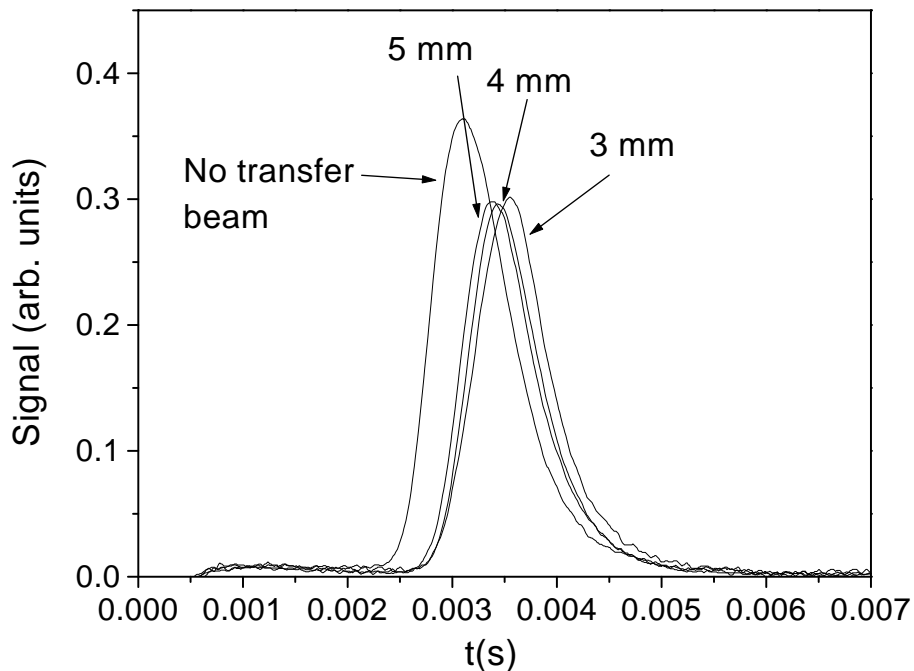


Fig. 4. Fluorescence signal measured for three indicated distances of the transfer beam from the MOT center. The peaks of the fluorescence curves arrive later as the transfer beam is moved closer to the MOT center.

## 5 Numerical Simulation

We have numerically simulated the dynamics of the MOT with the push and transfer beams using a classical description of the center-of-mass motion and a quantum-mechanical description of the internal dynamics of the atoms. We have used the analysis given in [8] as a starting point for our model. For a two-level system, the radiation pressure force acting on the atom due to a single laser beam is the product of the photon momentum multiplied by the photon scattering rate  $\Gamma_{\text{scatter}}$ , and is given by

$$\mathbf{F} = \hbar\mathbf{k}\Gamma_{\text{scatter}} = \hbar\mathbf{k}\frac{\Gamma}{2s+1}, \quad (1)$$

where  $\Gamma$  is the decay rate of the excited state and  $s$  is the saturation parameter

$$s = \frac{I}{I_{\text{sat}}} \frac{\Gamma^2}{\Gamma^2 + 4(\delta - \mathbf{k} \cdot \mathbf{v} - \Delta E_{\text{Zeeman}}/\hbar)^2}. \quad (2)$$

The saturation parameter takes into account the Doppler shift due to the (classical) atomic velocity  $\mathbf{v}$  as well as the relative Zeeman shift  $\Delta E_{\text{Zeeman}}$  between the involved states arising from the magnetic field of the MOT coils and the atom guide wires. Further,  $\delta$  is the field-free laser detuning,  $I$  the beam intensity, and  $I_{\text{sat}} = 1.6 \text{ mW/cm}^2$  the saturation intensity.

The  $F = 2 \rightarrow F' = 3$  MOT transition of  $^{87}\text{Rb}$  involves multiple magnetic sub-components with respective Zeeman shifts and Clebsch-Gordan coefficients. Further, to be able to calculate the average radiation pressure force, the probability distribution of the atom over the magnetic sublevels of the  $F = 2$  ground state needs to be determined. To make the model numerically more tractable, we use an  $F = 0 \rightarrow F' = 1$  model transition with wavelength and saturation intensity equal to those of the Rb D2 line, as explained in [8]. Also, due to the low density of atoms in MOTs designed to produce cold atomic beams, we can ignore collisions between atoms and simulate the dynamics of each particle independently.

Using these assumptions, the radiation-pressure force on an atom due to the MOT beams and the pusher beam becomes

$$\mathbf{F} = \sum_{i=1,7} \sum_{m=-1,1} \hbar \mathbf{k}_i \frac{\Gamma}{2} \frac{s_{i,m}}{1 + \sum_{i',m'} s_{i',m'}} \quad (3)$$

where

$$s_{i,m} = \frac{I_{i,m}}{I_{\text{sat}}} \frac{\Gamma^2}{\Gamma^2 + 4(\delta_i - \mathbf{k}_i \cdot \mathbf{v} + m\mu_B/\hbar)^2} \quad (4)$$

is the saturation parameter of the individual beam components. The  $i$  and  $m$  are indices for the beam number (six MOT beams plus one push beam) and the laser polarization, respectively. Each laser beam  $i$  is decomposed into its  $\sigma_-$ ,  $\pi$  and  $\sigma_+$  intensity components  $I_{i,-1}$ ,  $I_{i,0}$ , and  $I_{i,1}$  in a coordinate frame aligned with the magnetic-field direction at the (time-dependent) location of the atom. The denominator term  $1 + \sum_{i',m'} s_{i',m'}$  in Eq. 3 is introduced in order to obtain a reasonable saturation behavior [8] (the magnitude of the force on an atom must not exceed  $\hbar k \Gamma / 2$ ).

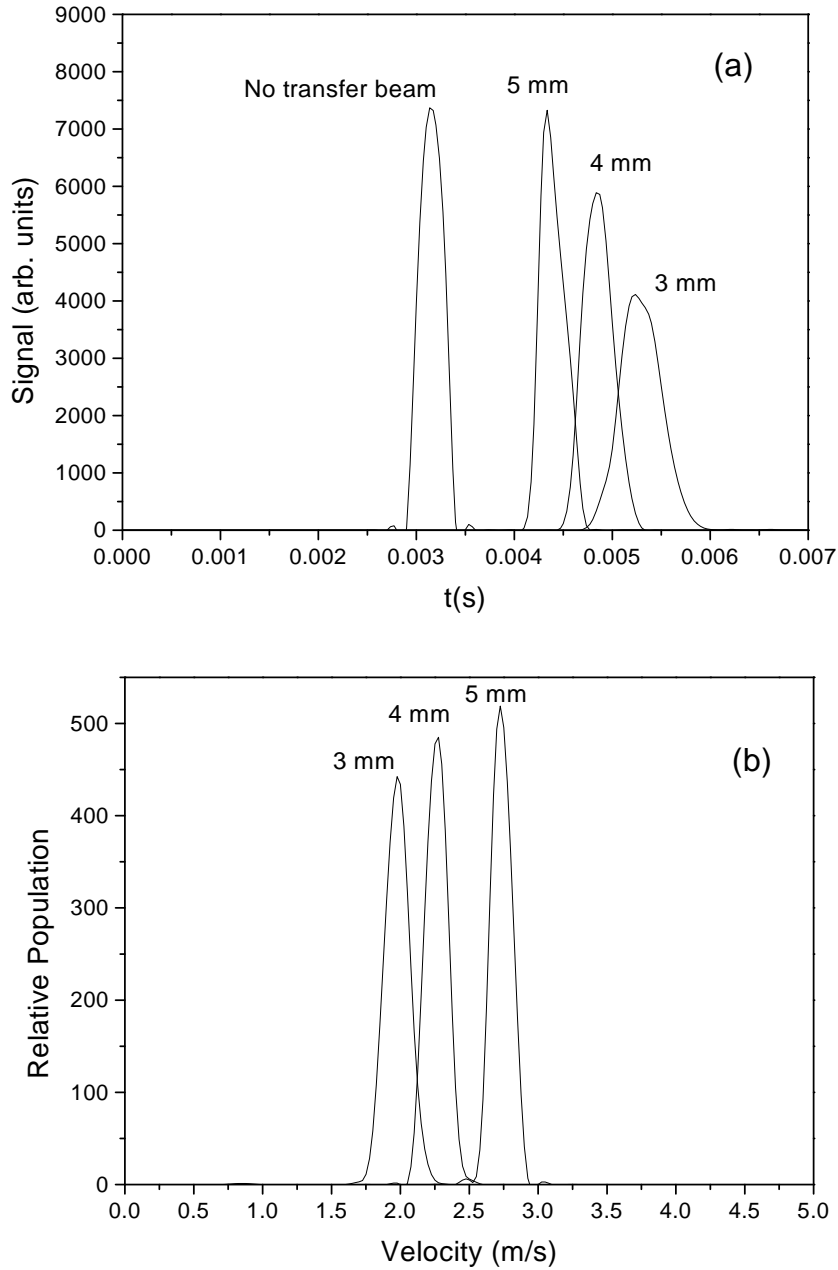


Fig. 5. (a) Simulated fluorescence signals corresponding to the experimental parameters in Fig. 4 for transfer beams at 3, 4 and 5 mm from the MOT center. Push beam intensity is  $8 \text{ mW/cm}^2$  and single-beam MOT intensity is  $5 \text{ mW/cm}^2$ . (b) Corresponding distributions of the velocity of atoms in the dark atomic beam.

In the following, we explain the features we have added to the model outlined in [8]. Spontaneous emission causes a diffusive motion in momentum space. In our model, we integrate, as the atom propagates, the total number of photons  $N$  that have been scattered. At suitable time intervals, a velocity kick of magnitude  $\sqrt{N}$  times the single-photon recoil velocity and with a random

direction is added to the velocity of the atom, and  $N$  is re-set to zero. We have verified that this procedure produces the expected steady-state temperature and cloud size of the MOT (with the push beam turned off). Further, in addition to the ground and excited states, we introduce a virtual dark state that the atom can be transferred to by a transfer beam. This state does not interact with the MOT or push beams. The role of the repumper is simulated by a transfer of atoms back to the  $F = 0$  state of the simulation. We ignore the momentum changes associated with the repumper and transfer beams because they amount to just a few photon recoils.

Fig. 5(a) shows the simulated fluorescence signals corresponding to the conditions for the data shown in Fig. 4. The calculations reproduce the qualitative features of the effect of the push beam position. The corresponding velocity distributions of the atoms are shown in Fig. 5(b). The simulations indicate a much lower beam velocity than the experimental data. This quantitative discrepancy can be attributed in part to imperfect beam geometries in the experiment, and, mostly, to repumper stray light scattered by the uncoated surfaces of our quartz vacuum chamber. The repumper stray light can re-pump atoms that have been transferred into the dark state back into the bright state and thereby make them susceptible to unwanted acceleration.

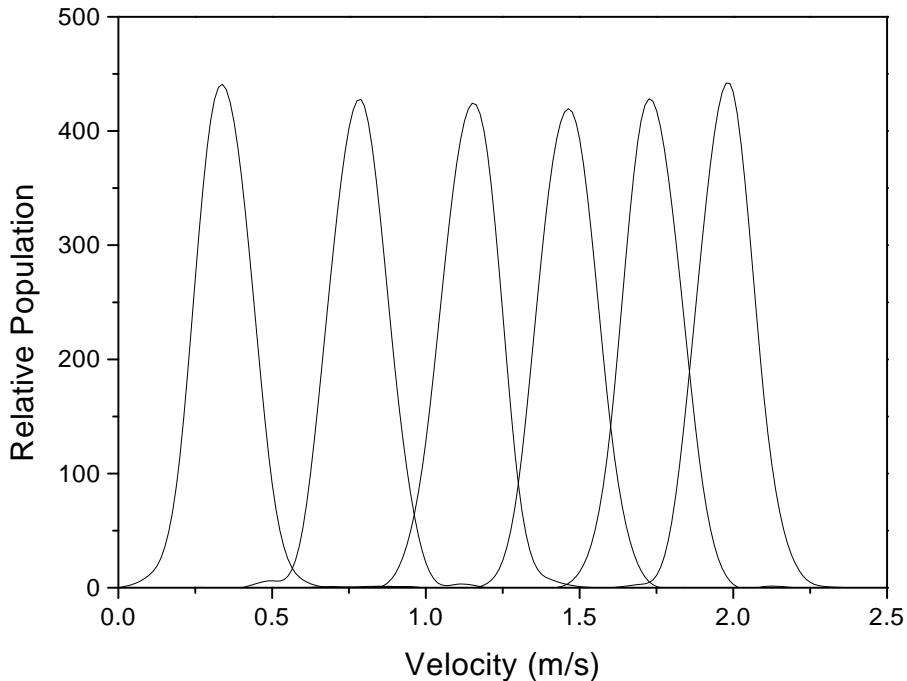


Fig. 6. Simulated velocity distributions for push beam intensities ranging from 3 to 8  $\text{mW}/\text{cm}^2$  (in steps of 1  $\text{mW}/\text{cm}^2$  from left to right) and a transfer beam located 3 mm from the MOT center. The single-beam MOT intensity is 5  $\text{mW}/\text{cm}^2$ .

The atomic beam velocity is sensitive to all laser beam parameters. In our

simulation, suitable parameters lead to dark atomic beams with velocities as slow as 0.3 m/s, which is about a factor 30 smaller than the method of the LVIS. A few simulated velocity distributions are shown in Fig. 6. There, the RMS velocity spread is of order 0.2 m/s in all cases. The slowest velocities are obtained using push beam intensity of 3 mW/cm<sup>2</sup> and a transfer beam separation from the MOT of 3 mm. While experimental limitations have prevented us from a quantitative reproduction of these theoretical results, we have been able to demonstrate the basic functionality of the technique.

## 6 Conclusion

We have experimentally demonstrated a simple technique to produce atomic beams with velocities and velocity spreads that are much smaller than that obtained from an LVIS. By pumping the atoms into a dark state, we have produced a slow, dark atomic beam that can be guided in a magnetic atom guide. Since the guided, dark atomic beam is not susceptible to stray light from the nearby MOT atom source, it can be operated continuously and concurrently with the MOT. Our numerical simulations show that the technique can produce dark atomic beams with velocities less than 0.2 m/s and velocity spreads comparable to that of a (doppler-limited) moving optical molasses. Our small vacuum chamber with uncoated windows has resulted in significant stray repumper light in the guide, which prevented us from observing the very slow velocities predicted by our simulations. This problem can, however, easily be alleviated using a larger vacuum chamber with fewer reflecting surfaces. We believe that dark, guided atomic beams are an ideal atom source for the realization of a continuous BEC in a magnetic atom guide.

## References

- [1] W. Ertmer R. Blatt, J. L. Hall and M. Zhu, *Phy. Rev. Lett.* **54** (1985) 996.
- [2] W. D. Phillips and H. Metcalf, *Phy. Rev. Lett.* **48** (1982) 596.
- [3] E. Riis, D. S. Weiss, K. A. Moler, and S. Chu, *Phy. Rev. Lett.* **64** (1990) 1658.
- [4] T. B. Swanson, N. J. Silva, S. K. Mayer, J. J. Maki and D. H. McIntyre, *J. Opt. Soc. Am. B* **13** (1996) 1833.
- [5] S. Weyers, E. Aucouturier, C. Valentin and N. Dimarcq, *Opt. Comm.* **143** (1997) 30.
- [6] P. Berthoud, A. Joyet, G. Dudle, N. Sagna and P. Thomann, *Europhys. Lett.* **41** (1998) 141.

- [7] Z. T. Lu, K. L. Corwin, M. J. Renn, M. H. Anderson, E. A. Cornell and C. E. Wieman, *Phy. Rev. Lett.* **77** (1996) 3331.
- [8] W. Wohlleben, F. Chevy, K. Madison and J. Dalibard, *Eur. Phys. J. D* **15** (2001) 237.
- [9] L. Cacciapuoti, A. Castrillo, M. de Angelis and G. M. Tino, *Eur. Phys. J. D* **15** (2001) 245.
- [10] N. H. Dekker, C. S. Lee, V. Lorent, J. H. Thywissen, S. P. Smith, M. Drndic, R. M. Westervelt and M. Prentiss, *Phy. Rev. Lett.* **84** (2000) 1124.
- [11] M. Key, I. G. Hughes, W. Rooijackers, B. E. Sauer, E. A. Hinds, D. J. Richardson and P. G. Kazansky, *Phy. Rev. Lett.* **84** (2000) 1371.
- [12] B. K. Teo and G. Raithel, *Phy. Rev. A* **63** (2001) 031402(R).
- [13] M. Vengalattore, W. Rooijackers and M. Prentiss *e-print physics/0106028*.
- [14] E. Mandonnet, A. Minguzzi, R. Dum, I. Carusotto, Y. Castin and J. Dalibard, *Eur. Phys. J. D* **10** (2000) 9.
- [15] A. P. Chikkatur, Y. Shin, A. E. Leanhardt, D. Kielpinski, E. Tsikata, T. L. Gustavson, D. E. Printchard and W. Ketterle, *Science* **296** (2002) 2193.
- [16] P. Cren, C. F. Roos, A. Aclan, J. Dalibard and D. Guéry-Odoelin *To be published in Eur. Phys. J. D* (2002).
- [17] B. K. Teo and G. Raithel, *Phy. Rev. A* **65** (2002) 051401(R).